# A Control Scheme for Monitoring Process Covariance Matrices with More Variables than Observations

Zhonghua Li [a,*], Fugee Tsung [b]

[a] *School of Statistics and Data Science and LPMC, Nankai University, Tianjin 300071, P.R.China*

[b] *Department of Industrial Engineering and Decision Analytics, The Hong Kong University of Science and Technology, Kowloon, Hong Kong*

**Abstract**

In this paper, we propose a new control chart that integrates a powerful high-dimensional covariance matrix test with the exponentially weighted moving average procedure for monitoring high-dimensional variability with individual observations. Design and implementation of the proposed chart are provided, including search algorithm and a table for the control limits, diagnostic aids after the signal, effect of misspecifying the in-control distribution and a bootstrap procedure. Monte-Carlo simulation results show that the new chart, with its powerful inherited properties, provides satisfactory performance in various cases, especially for covariance shifts that involve diagonal components. The application of the proposed method is illustrated with a real data example from a white wine production process.

*Key words:* Quality Control; Statistical Process Control; High Dimension; Individual Observation; Process Variability

* Corresponding author.
*Email address:* zli@nankai.edu.cn (Zhonghua Li).

# 1 Introduction

## *1.1 Motivating examples and challenges*

In recent years, there has been an intense interest in multivariate statistical process control (MSPC) charts in the statistical, quality assurance and reliability research literature. [1], [2] and [3] have all pointed out that MSPC charts are one of the most rapidly developing areas of statistical process control (SPC) and suggest that basic and applied research is needed on methods for monitoring multivariate variables. In many industrial, manufacturing and service applications, it is an important factor to improve the quality for successful business, and the quality of a product is often related to several correlated quality characteristics. With advances in data acquisition systems and computing technologies, MSPC charts can and should play a greater role in monitoring and improving manufacturing processes ([4, 5]). Given a multivariate process of interest, the process mean is typically monitored by the Hotelling's $T^2$ chart ([6, 7, 8]) and the process variability is usually monitored by a chart based on the determinant $|S|$ or/and the inverse $S^{-1}$ of the sample covariance matrix $S$ ([9, 10, 11, 12]). The process variability can also be monitored by a chart based on the likelihood ratio test (LRT), which also involves $|S|$, such as those of [13], [14], [15], [16] and [17]. [18] give a comprehensive review on MSPC charts developed between 1990 and 2005 and designed for monitoring changes in a covariance matrix.

In many areas, including signal processing, network security, image processing, genetics and other economic problems, however, practitioners are more interested in the case where the dimension $p$ is large or proportional to the sample size $n$. In the UCI Machine Learning Repository, the "Wine Quality Data Set" covers the period from May 2004 to February 2007 and contains a total of 4898 observations. It is publicly available from http://archive.ics.uci.edu/ml/datasets/Wine+Quality. The data were individually recorded by a computerized system ($n = 1$), which automatically manages the process of wine sample testing from producer requests to laboratory and sensory analysis. For each of these observations, there are $p = 11$ continuous variables (based on physicochemical tests) including fixed acidity, volatile acidity, citric acid, residual sugar, chlorides, free sulfur dioxide, total sulfur dioxide, density, pH, sulphates and alcohol (denoted by $\mathbf{y}_1, \mathbf{y}_2, \cdots, \mathbf{y}_{11}$, respectively). These variables are the major focus in white wine production and any value falling outside the specification limits will affect the quality of the white wine. Therefore, these variables must be carefully monitored and controlled in the production. Another categorical variable, quality, indicating the wine quality between 0 (bad) and 10 (excellent), is also provided based on sensory analysis. The goal of this data analysis is mainly to model and monitor wine quality based on physicochemical tests.

Interested readers are referred to [19] for more details.

[20] study this data set under the key assumption that the covariance matrix does not change. We believe monitoring the process covariance matrix is also of great importance, not only for this wine quality data set, but also in any control procedure. As [4] points out, "just as it is important to monitor the process mean vector, it is also important to monitor process variability". There exist many other examples similar to this one in the literature. In ambulatory monitoring, it is important to detect what caused covariance matrix components to change ([21]). In a wafer fabrication process, changes in the covariance matrix are usually caused by changes of raw materials, deterioration of key equipment, and incorrect setting of process parameters ([22]). In an important process for silicon wafer manufacturing called lapping, several correlated variables are considered to be critical factors that determine the uniformity of the thickness of a wafer and therefore must be closely monitored ([23]). In the health care industry, the foetal state may be determined using a technique called cardiotocography, which measures multiple features such as the number of accelerations per second and the number of foetal movements per second. Any significant deviation of the covariance matrix of those features from the normal state indicates that the foetus may have a health problem ([24]).

In general, constructing a proper covariance matrix monitoring scheme for data like those in the "Wine Quality Data Set" has some technical challenges: (i) Given a multivariate process of interest, the process covariance matrix is usually monitored by charts based on the determinant $|S|$ or/and the inverse $S^{-1}$ of the sample covariance matrix $S$. Neither of these is applicable, especially for high-dimensional processes (as $p > n$ in the "Wine Quality Data Set" ), because the sample covariance matrix cannot be estimated accurately and easily; (ii) most existing MSPC charts for covariance matrices are based on multiple observations at each time point, which may be unreasonable in some applications where sampling may be expensive, destructive or time consuming. In these cases, individual sampling (as $n = 1$ in the "Wine Quality Data Set") may be more appropriate; (iii) some MSPC covariance matrix detecting schemes based on penalization ([22, 23, 25, 26]) are computationally intensive.

Despite the importance of monitoring high-dimensional process covariance matrices with individual observations, effective and computational tractable monitoring schemes are rare as far as we know. The aim of this paper is to establish a control chart for monitoring process covariance matrices with individual observations.

When the dimension $p$ is large or proportional to the sample size $n$, the variability monitoring schemes based on $|S|$ or $S^{-1}$ are no longer applicable or give poor performance due to the singularity of the sample covariance. On the one hand, [27] show that $\sqrt{n/p}\ln(|S|) \to -\infty$ as $p \to \infty$, which will make the control limit too wide and will cause the methods of [10], [14], [15] and [16] to perform poorly for a large $p$. On the other hand, it is known that the covariance matrix will not have an inverse when $p$ is larger than $n$, which will make the methods of [9] and [12] no longer applicable. Thus a proper and efficient monitoring scheme that is suitable for this situation is highly desirable and is the objective of this paper.

When the dimension and the sample size are comparable, process shifts may occur in only a few of the variance and/or covariance elements. These shifts are known as sparse shifts in the statistical literature. Under these circumstances, more powerful MSPC charts are developed via penalization. [28], [29], [30] and [31] propose control charts for monitoring the process mean vector. Among others, [22] obtain the estimator of the inverse $\Omega$ of the covariance matrix as follows:

$$\hat{\Omega} = \arg\min_{\Omega>0}\{tr(\Omega S) - \ln|\Omega| + \rho||\Omega - I_p||_1\},$$

where $I_p$ is the identity matrix, $||A||_1 = \sum_{i=1}^{p}\sum_{j=1}^{p}|a_{ij}|$ for a matrix $A = (a_{ij})_{p\times p}$, $tr(A)$ is the trace of $A$, and $\rho$ is a data-dependent tuning parameter that can be tuned to achieve different levels of sparsity of the resulting $\hat{\Omega}$ and construct the LRT chart with the monitoring statistic $\ln|\hat{\Omega}| + tr(S) - tr(\hat{\Omega}S)$. [23] differ from [22] in that they penalize $||\Omega||_1$ instead of $||\Omega - I_p||_1$. With a similar estimator to [23], [25] and [26] propose the LRT statistic $tr(\hat{\Omega}^{-1}) - \ln|\hat{\Omega}^{-1}| - p$. By penalizing the mean vector and covariance matrix separately, [32] propose a generalized LRT chart for the mean vector and the covariance matrix, simultaneously.

As pointed out by [24], even though the charts based on penalization mentioned above are shown to perform well in many cases, the performance depends heavily on the choice of tuning parameter $\rho$, which plays a critical role in balancing the robustness and sensitivity of the charts against various shifts. This tuning parameter $\rho$, is, unfortunately, not easy to set, as the authors have also shown. To avoid having to set the tuning parameter, [24] propose a new control chart by integrating the classical $L_2$-norm-based test with a maximum-norm-based test. [33] propose an $L_1$-norm and an $L_2$-norm-based distance between diagonal elements of the estimators from their expected values based on [34]'s multivariate exponentially weighted mean squared error (MEWMS) chart and multivariate exponentially weighted moving variance (MEWMV) chart.

When the dimension is large relative to the sample size, [35] give a well-conditioned estimator for the covariance matrix. [36], [37], [38] and [39] give hypothesis tests for the covariance matrices when the dimension is large compared to the sample size. They study the asymptotic behaviors of these tests when $p \to \infty$. Motivated by [37], we propose a multivariate control chart for monitoring high-dimensional process covariance matrices based on integrating exponentially weighted moving average (EWMA) on-line monitoring with the statistic

$$W = \frac{1}{p}tr(S-I)^2 - \frac{p}{n}(\frac{1}{p}tr(S))^2 + \frac{p}{n}, \tag{1}$$

which is selected due to its ease of computation and high power in detecting out-of-control (OC) covariance matrices. Work based on trace of $S$ exist in the literature. [40] propose a variability control chart based on $tr(S^2)$ and $tr(S^4)$. [41] construct a control chart based on first taking the EWMA of the product of each observation and its transpose and computing the square distances between estimators and true parameters.

Our proposed chart has the following advantages: (i) Unlike the penalization-based charts, it circumvents the need to select a tuning parameter $\rho$; (ii) it is able to handle the case when the dimension $p$ is larger than the sample size $n$; (iii) it is able to handle the case when the sample size is one. The average run length (ARL), which is defined as the average number of samples before the control chart signals an OC condition ([4]), is employed as a criterion to study the properties of the new chart. We find that the new chart is sensitive in detecting changes in high-dimensional process covariance matrices, especially when shifts occur in the diagonal part of the covariance matrices.

The rest of this paper is organized as follows. In Section 2, our proposed control chart is presented. Design and implementation of the chart are provided in Section 3, including search algorithm and a table for the control limits, diagnostic aids after the signal, effect of misspecifying the in-control (IC) distribution and a bootstrap procedure. In Section 4, the performance of the proposed chart is evaluated using Monte Carlo simulations from the perspective of the ARL. The application of our proposed method is illustrated in Section 5 with a real data example from a white wine production process. In Section 6, the paper is concluded and future research directions are suggested.

## 2 A New Chart for Monitoring High-Dimensional Variability

### *2.1 Tests for the covariance matrix when p and n are comparable*

Assume that a process of interest consists of $p$ quality characteristics denoted by $\mathbf{X}$, where $\mathbf{X} \sim N_p(\boldsymbol{\mu}, \boldsymbol{\Sigma})$, a p-dimensional multivariate normal distribution with mean vector $\boldsymbol{\mu}$ and covariance matrix $\boldsymbol{\Sigma}$. Let $\mathbf{X}_t = \{\mathbf{X}_{t1}, \mathbf{X}_{t2}, \ldots, \mathbf{X}_{tn}\}, t = 1, 2, \ldots,$ be the $t^{th}$ sample of size $n$ drawn from the process, and let $\boldsymbol{\mu}_0$ and $\boldsymbol{\Sigma}_0$ be the desired mean vector and covariance matrix, respectively. Assume also that the random vectors $\mathbf{X}_{tj}$ are independent of each other, both within the samples and across the samples. Let

$$\bar{\mathbf{X}}_t = \sum_{j=1}^{n} \mathbf{X}_{tj}/n, \quad \mathbf{S}_t = \sum_{j=1}^{n} (\mathbf{X}_{tj} - \bar{\mathbf{X}}_t)'(\mathbf{X}_{tj} - \bar{\mathbf{X}}_t)/n \tag{2}$$

be the $t^{th}$ sample mean vector and sample covariance matrix, respectively.

To be more specific, assume that the $t^{th}$ future observation, $\mathbf{X}_t$, is collected over time from the following general multivariate change-point model:

$$\mathbf{X}_t \sim \begin{cases} N_p(\boldsymbol{\mu}_0, \boldsymbol{\Sigma}_0), & \text{if} \quad t = 0, 1, \ldots, \tau; \\ N_p(\boldsymbol{\mu}_1, \boldsymbol{\Sigma}_1), & \text{if} \quad t = \tau + 1, \ldots, \end{cases} \tag{3}$$

where $\tau$ is the unknown change point, $\boldsymbol{\mu}_0$ and $\boldsymbol{\mu}_1$ are the mean vectors, and $\boldsymbol{\Sigma}_1 \neq \boldsymbol{\Sigma}_0$ are the corresponding unknown shape matrices of parameters. As we are focusing on the Phase II on-line monitoring shifts of the process, $\boldsymbol{\mu}_0$ and $\boldsymbol{\Sigma}_0$ are assumed known or their values can be well estimated from a sufficiently large reference sample obtained at the end of Phase I study. When the process is IC, we assume, without loss of generality, that $\boldsymbol{\mu}_0 = \mathbf{0}$ and $\boldsymbol{\Sigma}_0 = \mathbf{I}_p$. Otherwise, the transformation of $\boldsymbol{\Sigma}_0^{-1/2}(\mathbf{X}_{tj} - \boldsymbol{\mu}_0)$ can be used instead of $\mathbf{X}_{tj}$. It should be pointed out that although our focus is on monitoring the covariance matrix, the mean vector may or may not change. Hence, the objective of this paper is to construct a control chart that not only can detect changes in the process variability but is also insensitive to shifts in the process mean.

The on-line monitoring problem (3) is closely related to statistical hypothesis testing for the one-sample variance problem in the context of multivariate statistical analysis. Hence, given a sample $\mathbf{X}_t$, the following hypothesis test is considered:

$$H_0 : \boldsymbol{\Sigma} = \mathbf{I}_p \quad \text{versus} \quad H_1 : \boldsymbol{\Sigma} \neq \mathbf{I}_p. \tag{4}$$

When the dimension $p$ is large compared to the sample size $n$, many hypothesis

tests exist for the covariance matrix, such as those of [36], [37], [38] and [39]. These papers study the asymptotic behaviors of these tests when $n \to \infty$ as well as $p \to \infty$. [36] proves that a test based on $V = \frac{1}{p}tr(S - I)^2$ is the locally most powerful invariant test for the hypothesis testing problem (4) when $n \to \infty$ while $p$ remains fixed. [37] show that $V$ is not consistent against every alternative when $p$ goes to infinity with $n$. They introduce the modified statistic $W$ as defined in (1). [37] prove that $W$ has the same $n$-asymptotic properties as $V$: it is $n$-consistent and has the same $n$-limiting distribution as $V$ under the null. But they also show that, contrary to $V$, the power and size of the test based on $W$ are robust against a large $p$, one that is even larger than $n$. Considering the ease of computation and high power of $W$ in detecting OC covariance matrices, we would like to construct a control chart by appropriately employing $W$.

### *2.2 A MEWMV control chart*

Although the monitoring problem (3) is closely related to the hypothesis testing problem (4), they are completely different and distinguished by the fundamental differences between on-line and off-line decision issues ([4]).

To construct a control chart by appropriately employing $W$ in (1), an estimator of the sample covariance matrix $S$ is needed. It seems that the sample covariance matrix $\mathbf{S}_t$ in (2) is an alternative. It is, however, cannot be employed directly for two reasons. First, even though the statistic $W$ is proposed when both $n \to \infty$ and $p \to \infty$, it is common in practice that only individual observations ($n = 1$) are available. In many industrial applications ([4], Chapter 6), due to practical and cost concerns, it may not be possible to collect more than one observation per sample. In these circumstances ($n = 1$), $\mathbf{S}_t$ in (2) will be a zero matrix and will not be well defined. Second, as the objective of this paper is to provide a control chart for monitoring the covariance matrix, it is expected that the proposed control chart will not be sensitive to the mean vector shifts. The $\mathbf{S}_t$ in (2) involves sample mean $\bar{\mathbf{X}}_t$ based only on the current sample at time $t$, so it will inevitably be influenced by changes in the mean vector.

To overcome this problem, motivated by [21] and [34], we replace the sample mean $\bar{\mathbf{X}}_t$ by an EWMA-type estimator. To be specific, two EWMA statistics based on the sample mean vector $\bar{\mathbf{X}}_t$ and sample covariance matrix $\mathbf{S}_t$ are given by

$$\begin{aligned} \mathbf{u}_t &= \lambda\bar{\mathbf{X}}_t + (1-\lambda)\mathbf{u}_{t-1}, \\ \mathbf{v}_t &= \lambda\mathbf{S}_t^* + (1-\lambda)\mathbf{v}_{t-1}, \end{aligned} \tag{5}$$

where $\mathbf{S}_t^* = \sum_{j=1}^{n}(\mathbf{X}_{tj} - \mathbf{u}_t)'(\mathbf{X}_{tj} - \mathbf{u}_t)/n$, $\mathbf{u}_0 = \mathbf{0}$, $\mathbf{v}_0 = \mathbf{I}_p$, and $\lambda$ is the smoothing parameter satisfying $0 < \lambda \leq 1$. It is well known that a smaller $\lambda$ leads to, generally, a quicker detection of smaller shifts ([42]).

Now it should be noted that the EWMA estimator of the process mean vector $\mathbf{u}_t$, rather than $\bar{\mathbf{X}}_t$, is used in the covariance matrix estimation. This estimator is expected to be more accurate as it uses sequentially updated estimates if the mean $\boldsymbol{\mu}_1$ deviates from $\boldsymbol{\mu}_0$. Therefore, the performance in detecting process changes, if any, may be improved. This kind of EWMA estimator is also suggested by [9] and [16].

Note also that in order to detect small or moderate covariance shifts effectively, we also incorporate the EWMA estimator $\mathbf{v}_t$ of the process covariance matrix $\mathbf{S}_t$. Here the EWMA strategy is not used directly to average the monitoring statistic but rather to obtain more precise estimates of the current process covariance matrix. This is analogous to the construction of multivariate EWMA control charts to some extent ([43]). [21] and [34] have shown that when estimating process variability based on individual observations, using EWMA to smooth the sample covariance matrix calculated from each individual observation is effective against process noise. The EWMA smoothing also has the effect of accumulating historical information for a more stable estimation.

Furthermore, as [16] and [34] have also pointed out, $\mathbf{v}_t$ is a positive definite matrix with probability 1 when $nt \geq p$, which implies that when $t > \frac{p}{n}$, $\mathbf{v}_t$ can be a reasonable estimate of $\boldsymbol{\Sigma}$. In this paper, we focus on $n = 1$ and $p \to \infty$, in which case $\frac{p}{n}$ may be so large that there does not exist a reasonable $t$ such that $\mathbf{v}_t$ is positive definite. Nevertheless, $\mathbf{v}_t$ is still employed as the estimate of $\boldsymbol{\Sigma}$ because the statistic $W$ only involves the trace, rather than inverse or determinant, of $S$. If a practitioner is still concerned about the singularity of $\mathbf{v}_t$, a well-conditioned estimator for covariance matrices proposed by [35] can be applied, where the estimator is the weighted sum of $\mathbf{v}_t$ and $\mathbf{I}_p$.

Under some mild conditions, as proved by [37], when the covariance matrix does not deviate from $\mathbf{I}_p$,

$$nW - p = \frac{n}{p}tr(S - \mathbf{I}_p)^2 - \frac{1}{p}(tr(S))^2 \xrightarrow{\mathcal{L}} N(1, 4), \tag{6}$$

as $n \to \infty$ and $p \to \infty$. Now we are ready to construct our control chart. By substituting $\mathbf{v}_t$ for $\mathbf{S}_t$ in (6) and dropping the normalizing constants, we obtain the monitoring statistic $T_t$ at time $t$, which is defined by

$$T_t = |tr(\mathbf{v}_t - \mathbf{I}_p)^2 - (tr(\mathbf{v}_t))^2|. \tag{7}$$

If $T_t > h$, an OC signal is given to indicate a covariance shift the process may have, where $h > 0$ is the control limit chosen to achieve a specified IC ARL

(denoted by $ARL_0$). In this paper, we call our proposed MEWMV-based chart for variability change with a large $p$ the MVP chart for short.

## 3 Design and Implementation of the MVP Chart

### *3.1 Determining parameters*

As we are using EWMA-type estimators of the mean vector and the covariance matrix, a smoothing constant $\lambda$ is involved. The effect of $\lambda$ in EWMA is well studied ([5]). In general, a smaller $\lambda$ leads to quicker detection of smaller shifts, which is still valid for our MVP. Based on our simulation results, we suggest choosing $\lambda \in [0.1, 0.2]$, which is a reasonable choice in practice ([16]).

To apply our MVP chart, the control limit $h$ should be determined first. Table 1 provides the control limits of the MVP chart for various combinations of $(\lambda, p, ARL_0)$. For other choices of parameters, a Fortran program for searching for the control limits is available from the authors upon request. A user can also code his own computer program in whichever software he wants to use (Python, R, Matlab, C++, and etc) by the guidelines below for finding $h$.

Step 1: Input parameters to be specified by the users, including $ARL_0$, dimension $p$ and smoothing parameter $\lambda$.

Step 2: Set the maximum of $h$ to $h_{max}$ such that the ARL value is larger than $ARL_0$ and the minimum of $h$ to $h_{min}$ such that the ARL value is smaller than $ARL_0$, and set $h = (h_{max} + h_{min})/2$.

Step 3: Set $\mathbf{u}_0 = \mathbf{0}$, $\mathbf{v}_0 = \mathbf{I}_p$ and $RL = 0$. Generate standard multivariate normal random vectors, update RL to $RL = RL + 1$ and compute $\mathbf{u}_1$, $\mathbf{v}_1$ to obtain $T_n$ until $T_n > h$.

Step 4: Repeat Step 3 $B$ times, which is the Monte Carlo sample size and obtain the average of the RL, i.e., ARL. If $ARL > ARL_0$, update $h_{max}$ to $h$; otherwise, update $h_{min}$ to $h$.

Step 5: The algorithm is not stopped until the absolute difference of $ARL$ and $ARL_0$ is less than a prefixed value $\varepsilon_1$ or the absolute difference of the current $h$ and the $h$ in the last iteration is less than another prefixed value $\varepsilon_2$.

Based on the search algorithm above, all the results are implemented in Fortran 95 with IMSL package. Routine "rnmvn" is used to generate standard multivariate normal random vectors. The computation time depends on the values of $B$, $\varepsilon_1$ and $\varepsilon_2$, as larger values of $B$ and smaller values of $\varepsilon_1$ and $\varepsilon_2$ will obtain more accurate results, but more time consuming, and vice versa. To balance the time and accuracy, we recommend that $B = 10000$, $\varepsilon_1 = 1$ and

$\varepsilon_2 = 10^{-2}$. The execution time is about several minutes on an Intel i5 with CPU processor 3.00 GHz.

**Insert Table 1 about here.**

The results displayed in Table 1 show stable and meaningful estimates of the control limits. We have chosen $\lambda = 0.1$ and $0.2$, $p = 5, 10, 20$ and $30$, and $ARL_0 = 200, 300, 370$ and $500$. From Table 1, we can see that for any given combination of $(p, \lambda)$, the higher the nominal $ARL_0$, the higher the value of $h$. Further, for a fixed $\lambda$, $h$ increases with the increase in $p$, and for a fixed $p$, $h$ decreases with the increase in $\lambda$.

### *3.2 Diagnostic aids*

When choosing a control chart to detect and eliminate special causes, a primary consideration should be the ability to signal quickly after a special cause occurs. Another important issue, particularly in the multivariate setting, is the development of procedures that can be employed after a signal for diagnostic purposes.

After a signal, it is important to know whether the shift is really an OC signal or a false alarm. As our MVP chart is on the basis of hypothesis test (4), it is difficult for us to identify whether the signal is real or not. We can only control the false alarm rate. Here, if we desire a lower false alarm rate, we set a larger $ARL_0$.

Assuming the signal is real, in order to identify the change point location, we propose using the maximum likelihood estimator (MLE) of the change point statistic. Assume that an OC is given at the $s^{th}$ observation by the MVP chart. The MLE $\hat{\tau}$ of the change point $\tau$ for a multivariate normal distribution is given by

$$\hat{\tau} = \arg_{0 \le j < s} \max \Big\{ \frac{1}{s-j} \sum_{t=j+1}^{s} (\bar{\mathbf{X}}_t - \mathbf{u}_t)' \mathbf{v}_t^{-1} (\bar{\mathbf{X}}_t - \mathbf{u}_t) \Big\}. \tag{8}$$

Note that this type of estimator has also been studied by [44] and [45].

After the change point location is identified, it is interesting to identify which variables, the mean vector or the covariance matrix, changed once the MVP chart signals. Note the objective of this paper is constructing control chart for covariance matrices that is insensitive to mean vector shifts. With this objective, we followed the technique of [21] and [34] to construct control chart for covariance matrices that is insensitive to mean vector shifts. So our MVP chart is not able to identify if mean vector changes.

It is also interesting to identify which components in the covariance matrix changed. A naive idea is to compare these components with those of $\mathbf{I}_p$, and those components with large difference are expected to be the changed components. It is, however, not easy to get the distribution of these components, hence not easy to get reliable diagnosis, which warrants further study.

### *3.3 Effect of misspecifying the IC distribution*

The construction of our proposed MVP chart is based on the assumption of multivariate normality. This claim is reasonable for some cases, it, however, may be troublesome for other cases, particularly as the number of variables (or dimensions) increases. It is interesting to study the effect of misspecifying the IC distribution on the MVP chart's ARLs relative to the ARLs obtained when the joint distribution of the variables is correctly specified.

We consider the multivariate $t$ distribution with $\nu$ degrees of freedom, denoted as $T_{p,\nu}$ and multivariate $\Gamma$ distribution with shape parameter $\nu$ and scale parameter 1, denoted as $\Gamma_{p,\nu}$. Many researchers propose and study multivariate $t$ distribution and multivariate $\Gamma$ distribution. Here we follow the definitions proposed by [46] and [47], respectively. Note $T_{p,\nu}$ and $\Gamma_{p,\nu}$ are selected to represent symmetric distributions with heavy tails and skewed distributions, respectively.

With control limits from Table 1, i.e., under the assumption of multivariate normality, the actual ARL values are shown in Figure 1 when the observations are generated from $T_{p,\nu}$ and $\Gamma_{p,\nu}$. The cases for $ARL_0$=200 and $p = 5, 10$ are considered. From Figure 1, it can be seen that (i) the actual ARL values of the MVP chart are smaller than the nominal $ARL_0$ value when $\nu$ is small, which implies that the related process would be stopped too often by the control chart and consequently a considerable amount of time and resource would be wasted in such cases; (ii) when $\nu$ is large, the actual ARL values of the MVP chart are comparable to the nominal $ARL_0$ value; (iii) when the dimension $p$ is larger, the effect is more severe. If one is concerned about the assumption of multivariate normality, a bootstrap procedure proposed in the next subsection can be employed.

**Insert Figure 1 about here.**

### *3.4 Bootstrap procedure*

As shown in the previous subsection, the MVP chart's ARLs would be affected if the IC distribution is not multivariate normal. In this case, the bootstrap

([48, 49]) is a widely accepted approach, such as [50] and [51] for univariate control charts, and [52] for multivariate control charts. The work of [53] based on supervised learning and [54] based on support vector data description may also shed light on directions to dealing with nonnormal variables.

To use the bootstrap method, we assume $m$ IC observations $\mathbf{Y} = \{\mathbf{Y}_1, \mathbf{Y}_2, \ldots, \mathbf{Y}_m\}$ are available to represent the IC distribution. By the bootstrap method, we first standardize the observations $\mathbf{Y}$ by the sample mean and sample covariance of $\mathbf{Y}$, and then repeatedly draw observations with replacement from the $m$ standardized observations, which are called the resampled data. The resampled data are used as Phase II observations to compute the values of $T_t$ in (7) of the MVP chart for any given $t$. Particularly, when determining the control limits, the difference lies in Step 3 of Section 3.1. Here, we repeatedly draw observations with replacement from standardized observations of $\mathbf{Y}$, rather than generating standard multivariate normal random vectors.

Such a bootstrap procedure would appear to be dependent on a large IC observations. This, however, may not always be available. It would be interesting to study when the bootstrap procedure could be considered, and what ARL performance can be expected from using this strategy. We study the effect of $m$ on the performance of MVP chart. To this end, we use $T_{p,\nu}$ and $\Gamma_{p,\nu}$ with $\nu = 5$, as well as $N_p(\mathbf{0}, \mathbf{I}_p)$. The cases for $ARL_0$=200 and $p = 5, 10$ are considered. Figure 2 shows the ARL values of MVP chart when the IC parameters $\boldsymbol{\mu}_0$ and $\boldsymbol{\Sigma}_0$ are computed from an IC data set with various historical sample sizes $m$. From Figure 2, it can be seen that (i) when $m$ is relatively small, the actual ARL values of the MVP chart are quite far away from the nominal level of 200; (ii) when $m$ increases, such biases decrease; (iii) when $m \geq 1000$, the ARL values become stable, which implies about 1000 samples are large enough; (iv) when the dimension $p$ is larger, more IC observations are needed.

**Insert Figure 2 about here.**

## 4 Comparison Studies

In this section, we give a brief introduction to the MaxNorm chart of [24], and we compare the performance of our MVP chart with the MaxNorm chart and some other competing charts, including the LASSO-MEWMC (LMC) chart of [22] and the penalized likelihood ratio (PLR) chart of [23]. Some alternative charts, such as those of [21] and [34], were compared with PLR or LMC and generally showed no better performance, and hence are not included here. Most of the other existing charts for monitoring the covariance matrix require $n > 1$, and they cannot be applied to our individual observation setting.

### *4.1 Existing work*

The LMC chart of [22] and the PLR chart of [23] were briefly introduced in Section 1.2. Now we will introduce the MaxNorm chart of [24].

In order to detect shifts that occur in a small number of elements of the covariance matrix, the MaxNorm chart proposed by [24] integrates the classical $L_2$-norm-based test with a maximum-norm-based test. The monitoring statistic at time $t$ is

$$T_{t_{MaxNorm}} = \max\left\{\frac{T_{t_1} - E(T_1)}{\sqrt{Var(T_1)}}, \frac{T_{t_2} - E(T_2)}{\sqrt{Var(T_2)}}\right\},$$

where

$$T_{t_1} = ||d_t||_2 = \sum_{i=1}^{p}\sum_{j=1}^{p} c_{t(ij)}^2, \quad T_{t_2} = ||d_t||_\infty = \max(|c_{t(11)}|, \ldots, |c_{t(pp)}|),$$

$d_t = (c_{t(11)}, c_{t(12)}, \ldots, c_{t(ij)}, \ldots, c_{t(pp)})'$, $c_{t(ij)}, i \leq j$, is an element of matrix $C_t = \Sigma_t - I_p$, $\Sigma_t = (1-\lambda)\Sigma_{t-1} + \lambda S_t$, $S_t = \sum_{j=1}^{n}(\mathbf{X}_{tj})'(\mathbf{X}_{tj})/n$, and $E(T_1)$, $E(T_2)$, $Var(T_1)$ and $Var(T_2)$ are the corresponding limits when $t \to \infty$.

As [24] point out, $T_{t_2}$ is more effective than $T_{t_1}$ if shifts occur in only a few elements in $\Sigma$. On the other hand, $T_{t_1}$ would outperform $T_{t_2}$ if shifts occur in a moderate to large number of covariance elements. Hence, combining these two statistics offers a more balanced detection ability.

### *4.2 ARL comparisons*

In this subsection, we compare the performance of the MVP chart, the MaxNorm chart of [24], the LMC chart of [22] and the PLR chart of [23] in terms of the OC ARL ($ARL_1$) as well as standard deviation of run length (SDRL) values. Following the simulations conducted in [24], [22] and [23], we set $\lambda = 0.1$ and the control limits such that the $ARL_0$ is approximately 200 for all charts. Note that when the process is IC, we assume $\boldsymbol{\mu}_0 = \mathbf{0}$ and $\boldsymbol{\Sigma}_0 = \mathbf{I}_p$. As the number and variety of OC settings are too large to allow a comprehensive comparison and it is almost impossible to include all possible OC scenarios in the simulation, considering our goal is to show the effectiveness and sensitivity of the MVP chart, we only choose certain representative models for illustration. Following the simulation settings of [24] and [23], we consider the following seven OC matrices: $\boldsymbol{\Sigma_1} = (1+\delta)I_p$,

$$\boldsymbol{\Sigma_2} = \begin{pmatrix} 1+\delta & & & \\ & 1 & & 0 \\ & & \ddots & \\ & 0 & & 1 \end{pmatrix}_{p\times p}, \quad \boldsymbol{\Sigma_3} = \begin{pmatrix} 1 & \delta & \delta & & \\ \delta & 1 & \delta & & 0 \\ \delta & \delta & 1 & & \\ & & & 1 & \\ & 0 & & & \ddots \\ & & & & & 1 \end{pmatrix}_{p\times p},$$

$$\boldsymbol{\Sigma_4} = \begin{pmatrix} 1 & \delta & & & \\ \delta & 1 & & 0 & \\ & & 1 & & \\ & 0 & & \ddots & \\ & & & & 1 \end{pmatrix}_{p\times p}, \quad \boldsymbol{\Sigma_5} = \begin{pmatrix} 1+\delta & \delta & \delta & & \\ \delta & 1+\delta & \delta & & 0 \\ \delta & \delta & 1+\delta & & \\ & & & 1 & \\ & 0 & & & \ddots \\ & & & & & 1 \end{pmatrix}_{p\times p},$$

$$\boldsymbol{\Sigma_6} = \begin{pmatrix} 1+\delta^2 & \delta & & & \\ \delta & 1+\delta^2 & & 0 & \\ & & 1 & & \\ & 0 & & \ddots & \\ & & & & 1 \end{pmatrix}_{p\times p}, \quad \boldsymbol{\Sigma_7} = \begin{pmatrix} 1+\delta & \delta & & & & \\ \delta & 1+\delta & & 0 & & \\ & & 1 & & & \\ & & & \ddots & & \\ & 0 & & 1 & & \\ & & & & 1+\delta & \delta \\ & & & & \delta & 1+\delta \end{pmatrix}_{p\times p}.$$

It should be noted that $\boldsymbol{\Sigma_2}$, $\boldsymbol{\Sigma_3}$, $\boldsymbol{\Sigma_4}$ and $\boldsymbol{\Sigma_6}$ are also studied in [22].

As pointed out by [24], the seven covariance matrices can be divided into three categories. Category I consists of $\boldsymbol{\Sigma_1}$ and $\boldsymbol{\Sigma_2}$, in which the shifts occur in just different diagonal elements. Category II includes $\boldsymbol{\Sigma_3}$ and $\boldsymbol{\Sigma_4}$, where the shifts occur in off-diagonal elements. Category III consists of $\boldsymbol{\Sigma_5}$, $\boldsymbol{\Sigma_6}$ and $\boldsymbol{\Sigma_7}$, where the shifts occur in both the diagonal and off-diagonal elements.

The $ARL_1$ and SDRL values of the MVP chart are obtained through Monte Carlo simulation with a simulation size of 10,000. The run length is sufficient long, enabling us to draw reasonable conclusions. The $ARL_1$ and SDRL values of the MaxNorm chart of [24], the LMC chart of [22] and the PLR chart of [23] are taken from Tables 4 and 5 of [24]. To evaluate the deviation of OC matrices

$\mathbf{\Sigma_i}, i = 1, \ldots, 7$ and IC matrix $\mathbf{\Sigma_0} = \mathbf{I}_p$, the $L_2$ matrix norm is employed, i.e.,

$$\Delta = ||\mathbf{\Sigma_i} - \mathbf{I}_p||_2,$$

where $||A||_2 = \sqrt{\sum_{i=1}^{p}\sum_{j=1}^{p} a_{ij}^2}$ for a matrix $A = (a_{ij})_{p\times p}$. For the PLR and LMC charts, different values of $\rho$ will have different detection performance. To show the influence of $\rho$, [23] studied $\rho$ in the interval $[0.05, 1.8]$ and [22] considered $\rho$ in the interval $[0.02, 1.2]$. From their simulations, too small a $\rho$ or too large a $\rho$ would bring poor performance in most cases. Therefore, three different $\rho$ values are chosen, i.e., $\rho = 0.05, 0.20, 1.00$, for better trade-off in different OC covariance matrices.

Table 2 shows the comparison results for $p = 5$, a dimension that is not too large. When the OC covariance matrix is $\mathbf{\Sigma_1}$, the MVP chart has the best performance among the existing charts, no matter what value of $\rho$ is used for PLR and LMC. The PLR and LMC charts perform better when a large tuning parameter $\rho$ was chosen, which forces more off-diagonal elements to zero and thus makes the PLR and LMC charts more sensitive to changes in variance components. The MaxNorm chart is never the best or the worst. As for $\mathbf{\Sigma_2}$, the MVP chart performs best when $\Delta$ is large, while LMC with $\rho = 1.00$ performs best when $\Delta$ is small. Note that $\mathbf{\Sigma_2}$ is an OC covariance matrix that is much more difficult to detect than $\mathbf{\Sigma_1}$, especially when $p$ is large.

**Insert Table 2 about here.**

In addition to using ARL as a performance measure, [55] propose a relative mean index (RMI) for evaluating the ARL performance of a control chart over a range of change magnitudes, which was also employed by [22]. The RMI is defined as

$$RMI = \frac{1}{d}\sum_{i=1}^{d}\frac{ARL_{\Delta_i} - ARL_{\Delta_i,\min}}{ARL_{\Delta_i,\min}},$$

where $ARL_{\Delta_i}$ is the $ARL_1$ under $\Delta_i$, $ARL_{\Delta_i,\min}$ is the minimum ARL for detecting a shift magnitude equal to $\Delta_i$ and $d$ is the number of different $\Delta_i$ considered. It can be seen that if the RMI of a given control chart is close to 0, then the control chart performs better in general than other charts over a range of change magnitudes. From Table 2, the RMI of the MVP chart is exactly 0 for $\mathbf{\Sigma_1}$, which indicates that this chart is the best performer in this setting. The RMI of the MVP chart is 0.14 for $\mathbf{\Sigma_2}$, a little larger than that of the MaxNorm chart.

When the OC covariance matrix is $\mathbf{\Sigma_3}$ or $\mathbf{\Sigma_4}$, the PLR chart with $\rho = 0.05$ or the LMC chart with $\rho = 0.05$ performs the best, which is expected since only the covariances have changed. The choice of smaller $\rho$ is expected since there are many non-zero entries in $\mathbf{\Sigma_3}$ and $\mathbf{\Sigma_4}$. The MaxNorm chart is still in between these charts in terms of performance. It should be pointed out that

although the proposed MVP chart can detect this kind of shifts, the performance is not satisfactory. $\mathbf{\Sigma_3}$ and $\mathbf{\Sigma_4}$ fall into Category II of the seven OC matrices, where the shifts occur in off-diagonal elements. From the monitoring statistics in (7), the MVP chart only makes use of the trace of $\mathbf{v}_t$, which is an estimator of the covariance matrix. This is the reason why the MVP chart performs unsatisfactorily under these circumstances.

When the OC covariance matrix is $\mathbf{\Sigma_5}$, which is similar to $\mathbf{\Sigma_3}$ but with added changes in the variance components, the changes in variances are likely to make the MVP chart more effective. As can be seen from Table 2, the MVP chart outperforms the other charts, except when $\Delta = 0.8$ for PLR with $\rho = 1.00$. In this case, the RMI of the MVP chart is 0.01, which is still the smallest. As for $\mathbf{\Sigma_6}$, the LMC chart with $\rho = 0.20$ performs the best when $\Delta$ is small, and the MVP chart performs the best when $\Delta$ is large. In this case, the RMI of the MVP chart is 0.15, which is still the smallest. In detecting $\mathbf{\Sigma_7}$, the MVP chart outperforms all other charts as expected. It is worth pointing out that the RMI of the MVP chart is exactly 0 for $\mathbf{\Sigma_7}$, which indicates that this chart is the best performer in this case.

In conclusion, when the dimension is not too large ($p = 5$ here), among the considered charts, the MVP chart is more effective if the process shifts cause changes in variance components, such as $\mathbf{\Sigma_1}$, $\mathbf{\Sigma_2}$, $\mathbf{\Sigma_5}$, $\mathbf{\Sigma_6}$ and $\mathbf{\Sigma_7}$. The MVP chart is less effective if shifts occur only in the off-diagonal components of the covariance matrix, such as $\mathbf{\Sigma_3}$ and $\mathbf{\Sigma_4}$.

Now we turn our attention to a high-dimensional case ($p = 30$). The comparison results are shown in Table 3. We emphasize the findings that are different from those for $p = 5$. Generally speaking, the performance of all charts deteriorates as $p$ increases. The performance of the MVP chart is less affected by the high dimensionality than the other charts. Note that when the dimension is high, the MVP chart gives the best performance for $\mathbf{\Sigma_1}$, $\mathbf{\Sigma_2}$, $\mathbf{\Sigma_5}$, $\mathbf{\Sigma_6}$ and $\mathbf{\Sigma_7}$; when the dimension is not so high, the MVP chart has the best performance for $\mathbf{\Sigma_1}$, $\mathbf{\Sigma_5}$, $\mathbf{\Sigma_6}$ and $\mathbf{\Sigma_7}$. It can therefore be concluded that the superiority of the MVP chart grows as $p$ increases. The MVP chart is particularly effective when the covariance changes occur in blocks in higher dimensions. Moreover, even for $\mathbf{\Sigma_4}$, for which only a small number of off-diagonal covariance matrix components change, the MVP chart performs the best when $\Delta = 2.0$. The RMI values of the MVP chart dropped from 4.71 and 4.41 to 0.44 and 0.73 for $\mathbf{\Sigma_3}$ and $\mathbf{\Sigma_4}$, respectively. In summary, when the dimension is high, the MVP chart not only retains the advantage of effectively detecting covariance shifts that involve diagonal components, but also satisfactorily detects shifts that involve only off-diagonal components.

**Insert Table 3 about here.**

As pointed out by an referee, the MVP chart statistic $T_t$ in (7) is based on the trace of $\mathbf{S}$. If a change in $\boldsymbol{\Sigma}$ causes the largest eigenvalue to increase by a factor $\delta$ while the smallest eigenvalue decreases by the same factor $\delta$, such as $\boldsymbol{\Sigma_8}$, the trace of $\mathbf{S}$ is unaltered. In general, the trace of $\mathbf{S}$ is effective for detecting increases in variance. However, if some components exhibit variance increases while others have compensating decreases, such as $\boldsymbol{\Sigma_9}$, the trace of $\mathbf{S}$ is unaltered, either. For these two cases, we found via simulation that our MVP chart is unable to detect these shifts, what ever $\delta$ is.

$$\boldsymbol{\Sigma_8} = \begin{pmatrix} 1+\delta & & & \\ & 1 & 0 & \\ & & \ddots & \\ 0 & & 1 & \\ & & & 1-\delta \end{pmatrix}_{p\times p}, \quad \boldsymbol{\Sigma_9} = \begin{pmatrix} 1+\delta & & & & \\ & 1+\delta & & 0 & \\ & & 1 & & \\ & & & \ddots & \\ & 0 & & 1 & \\ & & & & 1-\delta \\ & & & & & 1-\delta \end{pmatrix}_{p\times p}.$$

Although the PLR chart or the LMC chart with a properly chosen $\rho$ has the best performance in some cases, it is known that the choice of $\rho$ largely depends on the change patterns, which makes it difficult to recommend one $\rho$ value that works well for all OC settings. Furthermore, the construction of the PLR chart or the LMC chart involves a complex numerical minimization problem to obtain a sparse estimator of the sample covariance matrix. These problems do not apply to the MVP chart. Given its overall performance, the MVP chart is thus a good alternative for monitoring covariance matrices with individual observations, especially covariance shifts that involve diagonal components.

## 5 Real Data Example

In this section, we use the real "Wine Quality Data Set" from the motivating example in Section 1.1 to illustrate the application of our proposed MVP control chart.

[19] show that it is desirable to set up an on-line detection system to monitor the production process of Portuguese *Vinho Verde* wine to guarantee its quality. As mentioned in Section 2, the focus of this paper is on Phase II monitoring. Under the MSPC context of sequentially monitoring the wine production process, we assume that the standard quality level is 7 (LV7; as also suggested by [19]). The 880 observations of LV7 that are classified as IC

are used as the historical reference sample to estimate the mean vector and covariance matrix. The IC mean vector and covariance matrix, estimated from the 880 observations of LV7, are respectively

$$\boldsymbol{\mu}_0 = (6.73, 0.26, 0.33, 5.19, 0.04, 34.13, 125.11, 0.99, 3.21, 0.50, 11.37)$$

and

$$\boldsymbol{\Sigma_0} = \begin{pmatrix} 0.57 & -0.01 & 0.02 & 0.76 & 0.00 & -0.01 & 4.32 & 0.00 & -0.06 & -0.01 & -0.26 \\ -0.01 & 0.01 & 0.00 & -0.01 & 0.00 & -0.20 & -0.24 & 0.00 & 0.00 & 0.00 & 0.06 \\ 0.02 & 0.00 & 0.01 & 0.02 & 0.00 & 0.16 & 0.30 & 0.00 & 0.00 & 0.00 & -0.02 \\ 0.76 & -0.01 & 0.02 & 18.47 & 0.01 & 6.75 & 64.12 & 0.01 & -0.23 & -0.06 & -2.58 \\ 0.00 & 0.00 & 0.00 & 0.01 & 0.00 & 0.03 & 0.14 & 0.00 & 0.00 & 0.00 & -0.01 \\ -0.01 & -0.20 & 0.16 & 6.75 & 0.03 & 175.42 & 231.01 & 0.01 & 0.06 & 0.27 & -3.30 \\ 4.32 & -0.24 & 0.30 & 64.12 & 0.14 & 231.01 & 1072.10 & 0.05 & -0.16 & 0.04 & -18.99 \\ 0.00 & 0.00 & 0.00 & 0.01 & 0.00 & 0.01 & 0.05 & 0.00 & 0.00 & 0.00 & 0.00 \\ -0.06 & 0.00 & 0.00 & -0.23 & 0.00 & 0.06 & -0.16 & 0.00 & 0.03 & 0.00 & 0.02 \\ -0.01 & 0.00 & 0.00 & -0.06 & 0.00 & 0.27 & 0.04 & 0.00 & 0.00 & 0.02 & -0.01 \\ -0.26 & 0.06 & -0.02 & -2.58 & -0.01 & -3.30 & -18.99 & 0.00 & 0.02 & -0.01 & 1.55 \end{pmatrix}_{11\times 11}.$$

It can be seen that the sample covariance matrix $\boldsymbol{\Sigma_0}$ contains several large entries. For example, the covariance of $\mathbf{y}_6$ and $\mathbf{y}_7$ is 231.01. This demonstrates that the variables have considerable interrelationships and consequently a multivariate control chart is likely to be more appropriate than a set of univariate control charts.

Next, we assume that we have collected the LV6 observations sequentially. To demonstrate the application of the proposed MVP chart, we assume that the process covariance matrix has changed from $\boldsymbol{\Sigma_0}$ to $\boldsymbol{\Sigma_1}$. Furthermore, we set $\lambda = 0.1$ and the control limits such that the $ARL_0$ is approximately 500. Note that the IC covariance matrix of the transformed variable is simply the identity matrix $\mathbf{I}_{11}$. The step-by-step computation of the monitoring statistic is as follows.

Step 1: Set $t = 0$ and $\mathbf{u}_0 = \mathbf{0}$, $\mathbf{v}_0 = \mathbf{I}_{11}$.
Step 2: Update $t$ to $t = t + 1$. Read the $t^{th}$ observation $\mathbf{X}_t$ of LV6 and transform by $\boldsymbol{\Sigma}_0^{-1/2}(\mathbf{X}_t - \boldsymbol{\mu}_0)$.
Step 3: Compute $\mathbf{u}_t$ and $\mathbf{v}_t$ based on (5).
Step 4: Compute $T_t$ based on (7).
Step 5: Repeat Steps 2-4 until $T_t > h$.

Before process monitoring, the transformed observations of LV7 were investigated and found not to follow the multivariate normal distribution. In fact, the white wine data were also studied by [20] and [56], who showed that the P-values of the Shapiro-Wilk goodness-of-fit test for normality of the three variables $\mathbf{y}_2$, $\mathbf{y}_3$ and $\mathbf{y}_7$ were smaller than 0.0001, demonstrating that this data set is not multivariate normally distributed. Following the bootstrap procedure in Section 3.4, to determine the control limits, we calculate the charting statistics by randomly sampling the transformed observations of LV7 with replacement, instead of randomly generating multivariate normal variables. Through this bootstrap-type procedure, the control limit for the MVP chart is found to be 220.858. The monitoring statistics for the last 50 observations of LV7 and the first 23 observations of LV6, as well as the control limit, of the MVP chart are shown in Figure 3.

**Insert Figure 3 about here.**

From Figure 3, it can be seen that the monitoring statistics of the MVP chart exceed the control limit from approximately the $73^{rd}$ observation (the $23^{rd}$ LV6 observation), and the subsequent $T_t$ statistics are all well above the control limit. These signals are convincing enough, suggesting that a significant change in covariance has occurred. For this example data, as the last 50 observations are of LV7 and the first 23 observations are of LV6, and we assume that the standard quality level is LV7 (as also suggested by [19]), we can make sure the signal observed at the $73^{rd}$ observation is real. For comparison, [20] and [56] detect this change from the $25^{th}$ and $24^{th}$ LV6 observation, respectively, which are both later than our MVP chart. In order to identify the change point location, as our MVP chart gives an OC signal at the $73^{rd}$ observation, we obtain the MLE $\hat{\tau} = 58$ by (8).

Considering the ease of construction and efficient performance, the MVP chart should be a reasonable alternative for monitoring covariance matrices with individual observations.

## 6 Conclusions and Extensions

Motivated by [37], we propose a powerful high-dimensional control chart for monitoring process covariance matrices with more variables than observations based on integrating EWMA on-line monitoring with the statistic in (1). Due to the powerful properties of the test statistic and EWMA, the new chart provides satisfactory performance in various cases, especially for covariance shifts that involve diagonal components. Our proposed chart has the following advantages: (i) Unlike the penalization-based charts, it circumvents the need to select a tuning parameter $\rho$; (ii) it is able to handle the case when the

dimension $p$ is larger than the sample size $n$; (iii) it is able to handle the case when the sample size is one.

Compared with the MaxNorm chart of [24], the LMC chart of [22] and the PLR chart of [23], the proposed MVP chart is more effective if the process shifts cause changes in variance components, but less effective if shifts occur only in off-diagonal components of the covariance matrix when the dimension is not large. The performance of the MVP chart is, however, less affected by the high dimensionality than the other charts and the superiority of the MVP chart grows as $p$ increases. The MVP chart is particularly effective when the covariance changes occur in blocks in higher dimensions. Although the PLR chart or the LMC chart with proper $\rho$ displays the best performance in some cases, it is known that the choice of $\rho$ largely depends on the change patterns, which makes it difficult to recommend one $\rho$ value that works well for all OC settings. Furthermore, the construction of the PLR chart or the LMC chart involves a complex numerical minimization problem to obtain a sparse estimator of the sample covariance matrix. These problems do not apply to the MVP chart. Given its overall performance, the MVP chart is thus a good alternative for monitoring high-dimensional covariance matrices, especially covariance shifts that involve diagonal components.

It is worth pointing out here that the proposed MVP chart is studied and compared on the assumption that the parameters are exactly known when the process is IC. In some cases, the parameters may be unknown or many IC observations may be needed to estimate these parameters ([57, 58]). The performance of the MVP chart with estimated parameters warrants further study. Moreover, although a MLE of change point location of the proposed MVP chart is provided for diagnosis, more reliable diagnostic aids on identifying which components in the covariance matrix changed are needed. Furthermore, as the MVP chart is based on the trace, it is unable to detect shifts if some components exhibit variance increases while others have compensating decreases, which case also deserves further study.

## Acknowledgements

We would like to thank the editor and the two anonymous referees for their constructive comments and suggestions that have considerably improved this paper. This paper was supported by the National Natural Science Foundation of China (grants 11571191 and 11431006). Part of this paper was completed during Li's visit to the Department of Industrial Engineering and Decision Analytics at the Hong Kong University of Science and Technology, whose hospitality is appreciated.

## References


[1] S. Bersimis, S. Psarakis, and J. Panaretos. Multivariate statistical process control charts: An overview. *Quality and Reliability Engineering International*, 23(5):517–543, 2007.

[2] Vijay Kumar Butte and Loon Ching Tang. Multivariate charting techniques: A review and a line-column approach. *Quality and Reliability Engineering International*, 26(5):443–451, 2010.

[3] William H Woodall and Douglas C Montgomery. Some current directions in the theory and application of statistical process monitoring. *Journal of Quality Technology*, 46(1):78–94, 2014.

[4] Douglas C. Montgomery. *Introduction to Statistical Quality Control*. John Wiley and Sons, New York, 7th edition, 2013.

[5] Peihua Qiu. *Introduction to Statistical Process Control*. Chapman and Hall/CRC, Boca Raton, 2014.

[6] Yi Dai, Yunzhao Luo, Zhonghua Li, and Zhaojun Wang. A new adaptive cusum control chart for detecting the multivariate process mean. *Quality and Reliability Engineering International*, 27(7):877–884, 2011.

[7] Ross Sparks. Monitoring highly correlated multivariate processes using hotelling's $t^2$ statistic: Problems and possible solutions. *Quality and Reliability Engineering International*, 31(6):1089–1097, 2015.

[8] Galal M Abdella, Khalifa N Al-Khalifa, Sangahn Kim, Myong K Jeong, Elsayed A Elsayed, and Abdel Magid Hamouda. Variable selection-based multivariate cumulative sum control chart. *Quality and Reliability Engineering International*, 33(3):565–578, 2017.

[9] Arthur B Yeh, Dennis KJ Lin, Honghong Zhou, and Chandramouliswaran Venkataramani. A multivariate exponentially weighted moving average control chart for monitoring process variability. *Journal of Applied Statistics*, 30(5):507–536, 2003.

[10] Maman A Djauhari. Improved monitoring of multivariate process variability. *Journal of Quality Technology*, 37(1):32–39, 2005.

[11] Arsen Grigoryan and David He. Multivariate double sampling $|s|$ charts for controlling process variability. *International Journal of Production Research*, 43(4):715–730, 2005.

[12] Gemai Chen, Smiley W Cheng, and Hansheng Xie. A new multivariate control chart for monitoring both location and dispersion. *Communications in Statistics-Simulation and Computation*, 34(1):203–217, 2005.

[13] Joe H Sullivan and William H Woodall. Change-point detection of mean vector or covariance matrix shifts using multivariate individual observations. *IIE Transactions*, 32(6):537–549, 2000.

[14] Arthur B Yeh, Longcheen Huwang, and Yu-Fang Wu. A likelihood-ratio-based ewma control chart for monitoring variability of multivariate normal processes. *IIE Transactions*, 36(9):865–879, 2004.

[15] KD Zamba and Douglas M Hawkins. A multivariate change-point model for change in mean vector and/or covariance structure. *Journal of Quality*

*Technology*, 41(3):285–303, 2009.

[16] Jiujun Zhang, Zhonghua Li, and Zhaojun Wang. A multivariate control chart for simultaneously monitoring process mean and variability. *Computational Statistics and Data Analysis*, 54(10):2244–2252, 2010.

[17] Chia-Ling Yen, Jyh-Jen Horng Shiau, and Arthur B Yeh. Effective control charts for monitoring multivariate process dispersion. *Quality and Reliability Engineering International*, 28(4):409–426, 2012.

[18] Arthur B Yeh, Dennis KJ Lin, and Richard N McGrath. Multivariate control charts for monitoring covariance matrix: A review. *Quality Technology and Quantitative Management*, 3(4):415–436, 2006.

[19] Paulo Cortez, António Cerdeira, Fernando Almeida, Telmo Matos, and José Reis. Modeling wine preferences by data mining from physicochemical properties. *Decision Support Systems*, 47(4):547–553, 2009.

[20] Changliang Zou, Zhaojun Wang, and Fugee Tsung. A spatial rank-based multivariate ewma control chart. *Naval Research Logistics*, 59(2):91–110, 2012.

[21] Douglas M Hawkins and Edgard M Maboudou-Tchao. Multivariate exponentially weighted moving covariance matrix. *Technometrics*, 50(2):155–166, 2008.

[22] Arthur B Yeh, Bo Li, and Kaibo Wang. Monitoring multivariate process variability with individual observations via penalised likelihood estimation. *International Journal of Production Research*, 50(22):6624–6638, 2012.

[23] Bo Li, Kaibo Wang, and Arthur B Yeh. Monitoring the covariance matrix via penalized likelihood estimation. *IIE Transactions*, 45(2):132–146, 2013.

[24] Xiaobei Shen, Fugee Tsung, and Changliang Zou. A new multivariate ewma scheme for monitoring covariance matrices. *International Journal of Production Research*, 52(10):2834–2850, 2014.

[25] Edgard M Maboudou-Tchao and Norou Diawara. A lasso chart for monitoring the covariance matrix. *Quality Technology and Quantitative Management*, 10(1):95–114, 2013.

[26] Edgard M Maboudou-Tchao and Vincent Agboto. Monitoring the covariance matrix with fewer observations than variables. *Computational Statistics and Data Analysis*, 64:99–112, 2013.

[27] Zhidong Bai and Jack W Silverstein. Clt for linear spectral statistics of large-dimensional sample covariance matrices. *Annals of Probability*, 32(1):553–605, 2004.

[28] Kaibo Wang and Wei Jiang. High-dimensional process monitoring and fault isolation via variable selection. *Journal of Quality Technology*, 41(3):247–258, 2009.

[29] Giovanna Capizzi and Guido Masarotto. A least angle regression control chart for multidimensional data. *Technometrics*, 53(3):285–296, 2011.

[30] Changliang Zou, Wei Jiang, and Fugee Tsung. A lasso-based diagnostic framework for multivariate statistical process control. *Technometrics*,

53(3):297–309, 2011.

[31] Wei Jiang, Kaibo Wang, and Fugee Tsung. A variable-selection-based multivariate ewma chart for process monitoring and diagnosis. *Journal of Quality Technology*, 44(3):209–230, 2012.

[32] Kaibo Wang, Arthur B Yeh, and Bo Li. Simultaneous monitoring of process mean vector and covariance matrix via penalized likelihood estimation. *Computational Statistics and Data Analysis*, 78:206–217, 2014.

[33] Ahmad Ostadsharif Memar and Seyed Taghi Akhavan Niaki. New control charts for monitoring covariance matrix with individual observations. *Quality and Reliability Engineering International*, 25(7):821–838, 2009.

[34] Longcheen Huwang, Arthur B Yeh, and Chien-Wei Wu. Monitoring multivariate process variability for individual observations. *Journal of Quality Technology*, 39(3):258–278, 2007.

[35] Olivier Ledoit and Michael Wolf. A well-conditioned estimator for large-dimensional covariance matrices. *Journal of Multivariate Analysis*, 88(2):365–411, 2004.

[36] Hisao Nagao. On some test criteria for covariance matrix. *The Annals of Statistics*, 1(4):700–709, 1973.

[37] Olivier Ledoit and Michael Wolf. Some hypothesis tests for the covariance matrix when the dimension is large compared to the sample size. *The Annals of Statistics*, 30(4):1081–1102, 2002.

[38] Muni S Srivastava. Some tests concerning the covariance matrix in high dimensional data. *Journal of the Japan Statistical Society*, 35(2):251–272, 2005.

[39] James R Schott. A test for the equality of covariance matrices when the dimension is large relative to the sample sizes. *Computational Statistics and Data Analysis*, 51(12):6535–6542, 2007.

[40] Maman A Djauhari, Muhammad Mashuri, and Dyah E Herwindiati. Multivariate process variability monitoring. *Communications in Statistics-Theory and Methods*, 37(11):1742–1754, 2008.

[41] Arthur B Yeh, Longcheen Huwang, and Chien-Wei Wu. A multivariate ewma control chart for monitoring process variability with individual observations. *IIE Transactions*, 37(11):1023–1035, 2005.

[42] James M. Lucas and Michael S. Saccucci. Exponentially weighted moving average control schemes: Properties and enhancements. *Technometrics*, 32(1):1–12, 1990.

[43] Cynthia A. Lowry, William H. Woodall, Charles W. Champ, and Steven E. Rigdon. A multivariate exponentially weighted moving average control chart. *Technometrics*, 34(1):46–53, 1992.

[44] Changliang Zou and Fugee Tsung. Directional mewma schemes for multistage process monitoring and diagnosis. *Journal of Quality Technology*, 40(4):407–427, 2008.

[45] Joseph J Pignatiello Jr and Thomas R Samuel. Estimation of the change point of a normal process mean in spc applications. *Journal of Quality technology*, 33(1):82–95, 2001.

[46] Pi-Erh Lin. Some characterizations of the multivariate t distribution. *Journal of Multivariate Analysis*, 2(3):339–344, 1972.

[47] AM Mathal and PG Moschopoulos. A form of multivariate gamma distribution. *Annals of the Institute of Statistical Mathematics*, 44(1):97–106, 1992.

[48] B Efron. Bootstrap methods: Another look at the jackknife. *The Annals of Statistics*, 7(1):1–26, 1979.

[49] Bradley Efron and Robert J Tibshirani. *An Introduction to the Bootstrap*. Chapman and Hall/CRC, Boca Raton, 1994.

[50] Snigdhansu Chatterjee and Peihua Qiu. Distribution free cumulative sum control charts using bootstrap-based control limits. *Annals of Applied Statistics*, 3(1):349–369, 2009.

[51] Axel Gandy and Jan Terje Kvaløy. Guaranteed conditional performance of control charts via bootstrap methods. *Scandinavian Journal of Statistics*, 40(4):647–668, 2013.

[52] Poovich Phaladiganon, Seoung Bum Kim, Victoria CP Chen, Jun-Geol Baek, and Sun-Kyoung Park. Bootstrap-based $t^2$ multivariate control charts. *Communications in Statistics-Simulation and Computation*, 40(5):645–662, 2011.

[53] Walid Gani, Hassen Taleb, and Mohamed Limam. An assessment of the kernel-distance-based multivariate control chart through an industrial application. *Quality and Reliability Engineering International*, 27(4):391–401, 2011.

[54] Edgard M Maboudou-Tchao. Kernel methods for changes detection in covariance matrices. *Communications in Statistics-Simulation and Computation*, 47(6):1704–1721, 2018.

[55] Dong Han and Fugee Tsung. A reference-free cuscore chart for dynamic mean change detection and a unified framework for charting performance comparison. *Journal of the American Statistical Association*, 101(473):368–386, 2006.

[56] Zhonghua Li, Changliang Zou, Zhaojun Wang, and Longcheen Huwang. A multivariate sign chart for monitoring process shape parameters. *Journal of Quality Technology*, 45(2):149–165, 2013.

[57] Stelios Psarakis, Angeliki K Vyniou, and Philippe Castagliola. Some recent developments on the effects of parameter estimation on control charts. *Quality and Reliability Engineering International*, 30(8):1113–1129, 2014.

[58] Aya A Aly, Mahmoud A Mahmoud, and Ramadan Hamed. The performance of the multivariate adaptive exponentially weighted moving average control chart with estimated parameters. *Quality and Reliability Engineering International*, 32(3):957–967, 2016.

**Authors' Biographies**

Zhonghua Li is Associate Professor of the School of Statistics and Data Science, Nankai University. He received his PhD degree in statistics from Nankai University. His research interests include statistical process control and quality engineering. His research has been published in various refereed journals including *Technometrics, Journal of Quality Technology, Quality and Reliability Engineering International*, etc.

Fugee Tsung is Professor of the Department of Industrial Engineering and Decision Analytics (IEDA), Director of the Quality and Data Analytics Lab, at the Hong Kong University of Science & Technology (HKUST). He is a Fellow of the Institute of Industrial Engineers (IIE), Fellow of the American Society for Quality (ASQ), Fellow of the American Statistical Association (ASA), Academician of the International Academy for Quality (IAQ), and Fellow of the Hong Kong Institution of Engineers (HKIE). He is Editor-in-Chief of Journal of Quality Technology (JQT), Department Editor of IIE Transactions, and Associate Editor of Technometrics. He has authored over 100 refereed journal publications and was awarded the Best Paper Award from IIE Transactions in 2003, 2009, and 2017. He received both his M.Sc. and Ph.D. from the University of Michigan, Ann Arbor, and his B.Sc. from National Taiwan University. His research interests include quality engineering and management in manufacturing and service industries, statistical process control and monitoring, industrial statistics, and data analytics.

Table 1
The control limits of the MVP chart for various combinations of $(\lambda, p, ARL_0)$.

| | | $ARL_0$=200 | $ARL_0$=300 | $ARL_0$=370 | $ARL_0$=500 |
|---|---|---|---|---|---|
| $\lambda = 0.1$ | p=5 | 40.7031 | 42.1562 | 42.8906 | 44.0625 |
| | p=10 | 125.7812 | 128.8500 | 130.7812 | 133.0860 |
| | p=20 | 425.6248 | 431.0000 | 434.0624 | 438.4376 |
| | p=30 | 902.3436 | 908.4372 | 912.1872 | 917.3436 |
| $\lambda = 0.2$ | p=5 | 37.4219 | 39.0625 | 39.9219 | 41.1719 |
| | p=10 | 108.6250 | 111.3750 | 113.0000 | 115.1562 |
| | p=20 | 357.4220 | 361.5000 | 363.4376 | 366.5624 |
| | p=30 | 751.8750 | 758.6250 | 761.7186 | 765.3516 |

Figure captions:
Figure 1. Actual ARL values when the IC distribution is multivariate $T_{p,\nu}$ and $\Gamma_{p,\nu}$.
Figure 2. Actual ARL values when the IC distribution is multivariate $N_p(\mathbf{0}, \mathbf{I}_p)$, $T_{p,\nu}$ and $\Gamma_{p,\nu}$.
Figure 3. The monitoring statistics of the MVP chart applied to the white wine production process.

Table 2
ARL (SDRL) comparison when $n = 1, p = 5$. (Note: The ARL (SDRL) values of the PLR, LMC and MaxNorm charts are taken from Tables 4 and 5 of [24].)

| | $\Delta$ | PLR with $\rho$ | | | LMC with $\rho$ | | | MaxNorm | MVP |
|---|---|---|---|---|---|---|---|---|---|
| | | 0.05 | 0.20 | 1.00 | 0.05 | 0.20 | 1.00 | | |
| $\mathbf{\Sigma_1}$ | 0.8 | 27.9 | 21.3 | 14.5 | 28.3 | 22.4 | 21.9 | 18.6 | **12.7** |
| | | (22.7) | (17.1) | (11.5) | (23.1) | (17.9) | (18.6) | (15.7) | (12.6) |
| | 1.2 | 20.4 | 15.9 | 11.2 | 21.2 | 16.8 | 16.4 | 14.3 | **7.46** |
| | | (15.7) | (12.2) | (8.59) | (16.4) | (13.0) | (13.4) | (11.4) | (6.79) |
| | 1.6 | 16.8 | 13.1 | 9.33 | 17.2 | 14.0 | 13.6 | 11.7 | **5.24** |
| | | (12.7) | (9.72) | (7.02) | (13.1) | (10.4) | (10.9) | (9.10) | (4.40) |
| | 2.0 | 14.6 | 11.3 | 8.05 | 14.6 | 11.8 | 12.0 | 10.2 | **4.12** |
| | | (10.8) | (8.47) | (6.00) | (10.7) | (8.78) | (9.43) | (7.89) | (3.31) |
| | RMI | 1.92 | 1.26 | 0.59 | 1.97 | 1.39 | 1.36 | 1.02 | 0.00 |
| $\mathbf{\Sigma_2}$ | 0.8 | 40.3 | 34.0 | 28.2 | 42.2 | 37.0 | **26.2** | 27.3 | 37.5 |
| | | (33.2) | (28.2) | (24.7) | (34.5) | (30.7) | (22.8) | (23.7) | (40.1) |
| | 1.2 | 31.7 | 26.6 | 22.1 | 32.2 | 29.2 | **20.3** | 20.8 | 22.9 |
| | | (24.6) | (21.5) | (19.1) | (25.6) | (24.0) | (17.2) | (17.5) | (24.7) |
| | 1.6 | 26.4 | 22.7 | 18.2 | 27.0 | 24.5 | 17.0 | 17.4 | **16.2** |
| | | (20.6) | (18.0) | (15.4) | (20.5) | (19.4) | (14.3) | (14.5) | (17.0) |
| | 2.0 | 23.4 | 19.5 | 16.1 | 23.7 | 21.4 | 14.7 | 15.4 | **12.3** |
| | | (17.9) | (14.9) | (13.2) | (17.8) | (16.8) | (12.3) | (12.8) | (12.7) |
| | RMI | 0.66 | 0.40 | 0.15 | 0.70 | 0.53 | 0.06 | 0.10 | 0.14 |
| $\mathbf{\Sigma_3}$ | 0.8 | **47.8** | 52.5 | 153 | 48.2 | 48.3 | 143 | 79.8 | 196 |
| | | (36.5) | (43.5) | (153) | (37.4) | (39.4) | (137) | (73.5) | (209) |
| | 1.2 | 36.2 | 39.7 | 137 | **35.9** | 36.2 | 124 | 59.9 | 196 |
| | | (26.5) | (31.6) | (134) | (25.1) | (27.5) | (116) | (54.4) | (215) |
| | 1.6 | 29.6 | 32.3 | 123 | **29.2** | 29.8 | 107 | 49.3 | 195 |
| | | (19.5) | (24.4) | (120) | (19.4) | (21.9) | (101) | (43.8) | (218) |
| | 2.0 | **24.9** | 27.5 | 115 | 25.1 | 25.6 | 92.8 | 41.2 | 164 |
| | | (15.6) | (19.8) | (112) | (16.1) | (18.7) | (84.9) | (35.7) | (191) |
| | RMI | 0.01 | 0.10 | 2.96 | 0.00 | 0.02 | 2.46 | 0.67 | 4.71 |
| $\mathbf{\Sigma_4}$ | 0.8 | 36.7 | 45.3 | 129 | **36.4** | 38.5 | 75.3 | 86.9 | 198 |
| | | (23.2) | (34.8) | (127) | (22.9) | (27.9) | (65.7) | (80.8) | (217) |
| | 1.2 | 24.5 | 30.1 | 101 | **24.3** | 26.1 | 47.7 | 64.8 | 196 |
| | | (11.7) | (19.1) | (96.7) | (11.5) | (16.1) | (40.0) | (57.7) | (220) |
| | 1.6 | 18.3 | 22.1 | 82.7 | **18.1** | 19.8 | 34.8 | 49.9 | 104 |
| | | (6.53) | (11.4) | (77.5) | (6.53) | (10.4) | (26.6) | (42.9) | (122) |
| | 2.0 | **14.7** | 17.4 | 66.8 | 14.8 | 16.1 | 27.5 | 40.5 | 35.2 |
| | | (4.14) | (7.30) | (60.8) | (4.25) | (7.62) | (19.6) | (33.2) | (41.9) |
| | RMI | 0.01 | 0.22 | 3.20 | 0.00 | 0.08 | 0.96 | 1.64 | 4.41 |
| $\mathbf{\Sigma_5}$ | 0.8 | 41.1 | 35.8 | **35.0** | 41.2 | 35.3 | 42.6 | 36.5 | 36.9 |
| | | (34.1) | (30.1) | (31.6) | (33.9) | (28.9) | (39.1) | (32.4) | (39.6) |
| | 1.2 | 31.9 | 28.0 | 27.4 | 32.2 | 28.1 | 33.5 | 27.7 | **23.1** |
| | | (25.1) | (22.6) | (23.9) | (25.4) | (22.8) | (29.6) | (23.7) | (24.7) |
| | 1.6 | 26.6 | 23.2 | 23.1 | 26.9 | 23.7 | 27.7 | 22.9 | **16.4** |
| | | (20.5) | (18.6) | (19.8) | (20.7) | (18.6) | (24.3) | (19.7) | (17.2) |
| | 2.0 | 23.0 | 20.3 | 20.1 | 23.5 | 20.2 | 24.1 | 20.3 | **12.3** |
| | | (17.2) | (16.0) | (17.3) | (17.6) | (15.4) | (20.8) | (17.2) | (12.8) |
| | RMI | 0.51 | 0.33 | 0.31 | 0.53 | 0.33 | 0.58 | 0.32 | 0.01 |
| $\mathbf{\Sigma_6}$ | 0.8 | 43.0 | 40.1 | 47.1 | 42.8 | **39.2** | 48.6 | 44.6 | 61.1 |
| | | (34.0) | (33.0) | (43.2) | (33.7) | (32.0) | (43.9) | (40.6) | (67.7) |
| | 1.2 | 32.7 | 30.2 | 33.5 | 33.2 | **29.7** | 34.7 | 32.2 | 30.4 |
| | | (25.2) | (24.7) | (30.1) | (26.0) | (23.5) | (30.5) | (27.5) | (33.4) |
| | 1.6 | 27.4 | 24.4 | 26.3 | 27.5 | 24.8 | 27.3 | 25.3 | **17.9** |
| | | (20.4) | (19.2) | (23.1) | (21.2) | (19.4) | (23.2) | (21.4) | (19.2) |
| | 2.0 | 23.7 | 21.0 | 21.7 | 23.9 | 21.5 | 22.6 | 21.1 | **12.4** |
| | | (17.7) | (16.3) | (18.7) | (17.6) | (16.5) | (19.0) | (17.9) | (12.6) |
| | RMI | 0.41 | 0.27 | 0.39 | 0.42 | 0.28 | 0.44 | 0.33 | 0.15 |
| $\mathbf{\Sigma_7}$ | 0.8 | 34.9 | 28.9 | 24.5 | 35.2 | 29.8 | 33.5 | 28.3 | **24.0** |
| | | (27.3) | (23.7) | (21.1) | (28.1) | (24.2) | (29.9) | (23.7) | (24.8) |
| | 1.2 | 26.8 | 22.6 | 19.3 | 26.9 | 23.1 | 25.6 | 21.7 | **14.2** |
| | | (20.9) | (17.8) | (16.2) | (20.8) | (18.0) | (21.9) | (18.1) | (14.3) |
| | 1.6 | 22.5 | 18.5 | 15.8 | 22.3 | 18.9 | 21.4 | 18.2 | **9.86** |
| | | (16.8) | (14.0) | (12.7) | (16.9) | (14.3) | (18.0) | (14.9) | (9.46) |
| | 2.0 | 19.3 | 16.3 | 13.8 | 19.3 | 16.8 | 18.7 | 15.5 | **7.53** |
| | | (14.1) | (12.3) | (11.1) | (14.0) | (12.8) | (15.3) | (12.4) | (7.01) |
| | RMI | 1.05 | 0.71 | 0.45 | 1.05 | 0.75 | 0.96 | 0.65 | 0.00 |

Table 3
ARL (SDRL) comparison when $n = 1, p = 30$. (Note: The ARL (SDRL) values of the PLR, LMC and MaxNorm charts are taken from Tables 4 and 5 of [24].)

| | $\Delta$ | PLR with $\rho$ | | | LMC with $\rho$ | | | MaxNorm | MVP |
|---|---|---|---|---|---|---|---|---|---|
| | | 0.05 | 0.20 | 1.00 | 0.05 | 0.20 | 1.00 | | |
| $\mathbf{\Sigma_1}$ | 0.8 | 40.7 | 25.9 | 14.6 | 38.4 | 25.3 | 33.5 | 25.1 | **3.16** |
| | | (24.1) | (15.1) | (9.73) | (21.1) | (14.1) | (28.2) | (18.7) | (8.08) |
| | 1.2 | 32.5 | 20.4 | 11.4 | 31.4 | 19.9 | 25.3 | 18.7 | **1.74** |
| | | (17.0) | (10.9) | (7.06) | (15.6) | (10.1) | (20.2) | (12.9) | (3.20) |
| | 1.6 | 27.6 | 17.3 | 9.47 | 26.9 | 17.1 | 20.5 | 15.5 | **1.31** |
| | | (13.3) | (8.23) | (5.61) | (12.2) | (7.77) | (15.7) | (9.87) | (1.54) |
| | 2.0 | 24.4 | 15.2 | 8.13 | 24.1 | 15.2 | 17.9 | 13.3 | **1.16** |
| | | (10.4) | (6.73) | (4.69) | (9.73) | (6.48) | (13.4) | (8.13) | (0.89) |
| | RMI | 17.42 | 10.56 | 5.35 | 16.88 | 10.40 | 13.06 | 9.50 | 0.00 |
| $\mathbf{\Sigma_2}$ | 0.8 | 107 | 92.1 | 60.1 | 112 | 107 | 50.4 | **44.5** | 59.3 |
| | | (82.2) | (75.9) | (54.1) | (86.0) | (90.0) | (44.0) | (39.2) | (162) |
| | 1.2 | 91.3 | 77.3 | 47.0 | 98.1 | 92.1 | 37.5 | **33.2** | 34.7 |
| | | (67.8) | (60.9) | (40.9) | (73.8) | (76.3) | (32.6) | (27.8) | (96.3) |
| | 1.6 | 80.9 | 67.2 | 39.2 | 87.0 | 82.5 | 30.6 | 26.9 | **21.3** |
| | | (58.8) | (52.7) | (32.6) | (64.2) | (67.5) | (25.9) | (22.2) | (60.3) |
| | 2.0 | 73.1 | 60.1 | 35.0 | 78.9 | 72.5 | 26.0 | 22.8 | **15.0** |
| | | (50.6) | (45.8) | (28.7) | (55.3) | (57.2) | (21.3) | (18.7) | (42.2) |
| | RMI | 2.46 | 1.89 | 0.73 | 2.70 | 2.47 | 0.36 | 0.20 | 0.09 |
| $\mathbf{\Sigma_3}$ | 0.8 | **145** | 151 | 189 | 147 | 149 | 170 | 176 | 194 |
| | | (119) | (133) | (184) | (123) | (132) | (163) | (168) | (468) |
| | 1.2 | **125** | 133 | 181 | 126 | 134 | 157 | 163 | 189 |
| | | (102) | (113) | (176) | (100) | (115) | (148) | (158) | (461) |
| | 1.6 | **113** | 116 | 172 | 115 | 121 | 142 | 151 | 160 |
| | | (86.9) | (99.0) | (167) | (88.8) | (104) | (139) | (142) | (398) |
| | 2.0 | **102** | 104 | 165 | **102** | 108 | 128 | 143 | 152 |
| | | (77.3) | (86.3) | (158) | (76.1) | (91.5) | (121) | (135) | (384) |
| | RMI | 0.00 | 0.04 | 0.47 | 0.01 | 0.06 | 0.23 | 0.31 | 0.44 |
| $\mathbf{\Sigma_4}$ | 0.8 | 127 | 132 | 174 | 128 | 131 | **116** | 169 | 197 |
| | | (101) | (114) | (169) | (100) | (115) | (107) | (164) | (492) |
| | 1.2 | 99.3 | 107 | 156 | 98.8 | 100 | **77.7** | 138 | 179 |
| | | (71.6) | (88.9) | (150) | (70.8) | (82.2) | (67.1) | (132) | (454) |
| | 1.6 | 74.2 | 85.4 | 140 | 70.8 | 71.4 | **57.0** | 109 | 110 |
| | | (47.1) | (65.3) | (132) | (42.4) | (50.8) | (45.8) | (101) | (281) |
| | 2.0 | 51.2 | 67.1 | 122 | 43.0 | 43.0 | 42.8 | 86.1 | **40.4** |
| | | (23.3) | (46.7) | (113) | (13.8) | (20.1) | (32.8) | (77.1) | (113) |
| | RMI | 0.24 | 0.42 | 1.25 | 0.17 | 0.18 | 0.01 | 0.82 | 0.73 |
| $\mathbf{\Sigma_5}$ | 0.8 | 108 | 93.8 | 74.2 | 109 | 97.3 | 81.7 | 85.9 | **59.4** |
| | | (84.1) | (76.9) | (67.2) | (84.8) | (80.6) | (74.1) | (79.1) | (161) |
| | 1.2 | 93.8 | 79.5 | 60.1 | 94.7 | 86.2 | 62.2 | 67.7 | **34.4** |
| | | (70.0) | (63.6) | (54.1) | (70.4) | (70.6) | (55.8) | (60.8) | (98.0) |
| | 1.6 | 81.6 | 69.9 | 51.2 | 84.1 | 76.0 | 50.7 | 57.6 | **22.0** |
| | | (58.4) | (53.9) | (45.0) | (61.2) | (60.1) | (44.1) | (50.7) | (64.1) |
| | 2.0 | 73.9 | 61.6 | 44.4 | 76.3 | 68.9 | 42.8 | 49.2 | **15.2** |
| | | (50.9) | (46.1) | (38.3) | (52.6) | (53.5) | (37.1) | (42.8) | (43.6) |
| | RMI | 2.28 | 1.78 | 1.06 | 2.36 | 2.03 | 1.08 | 1.32 | 0.00 |
| $\mathbf{\Sigma_6}$ | 0.8 | 118 | 108 | 92.4 | 119 | 112 | **82.8** | 102 | 88.7 |
| | | (93.7) | (92.5) | (84.4) | (92.9) | (94.7) | (75.4) | (95.1) | (238) |
| | 1.2 | 98.0 | 88.4 | 69.6 | 102 | 95.4 | 58.8 | 73.5 | **46.2** |
| | | (74.0) | (72.6) | (63.2) | (78.1) | (78.3) | (51.8) | (66.6) | (129) |
| | 1.6 | 86.4 | 74.5 | 55.2 | 90.0 | 81.7 | 46.0 | 56.6 | **24.5** |
| | | (62.9) | (59.1) | (48.8) | (65.9) | (64.4) | (39.6) | (49.4) | (68.1) |
| | 2.0 | 77.7 | 64.7 | 45.4 | 80.6 | 74.0 | 37.5 | 45.6 | **14.6** |
| | | (55.1) | (49.8) | (39.1) | (58.0) | (58.2) | (31.8) | (39.8) | (43.4) |
| | RMI | 2.10 | 1.67 | 1.00 | 2.21 | 1.96 | 0.68 | 1.06 | 0.02 |
| $\mathbf{\Sigma_7}$ | 0.8 | 96.5 | 78.3 | 57.3 | 96.2 | 83.5 | 68.0 | 68.2 | **39.3** |
| | | (74.4) | (63.6) | (50.2) | (72.2) | (69.2) | (62.1) | (62.0) | (109) |
| | 1.2 | 80.1 | 64.3 | 45.2 | 82.1 | 70.6 | 52.0 | 52.7 | **19.7** |
| | | (57.5) | (48.5) | (39.5) | (59.6) | (54.7) | (46.3) | (46.1) | (57.9) |
| | 1.6 | 70.0 | 55.3 | 36.8 | 73.2 | 61.3 | 41.9 | 43.4 | **11.4** |
| | | (47.1) | (41.0) | (30.8) | (50.5) | (46.1) | (35.6) | (36.8) | (33.8) |
| | 2.0 | 62.4 | 49.4 | 31.7 | 65.3 | 54.8 | 35.0 | 37.2 | **7.56** |
| | | (40.4) | (35.0) | (25.4) | (43.5) | (40.5) | (28.6) | (31.4) | (21.6) |
| | RMI | 4.23 | 3.16 | 1.79 | 4.42 | 3.58 | 2.17 | 2.28 | 0.00 |

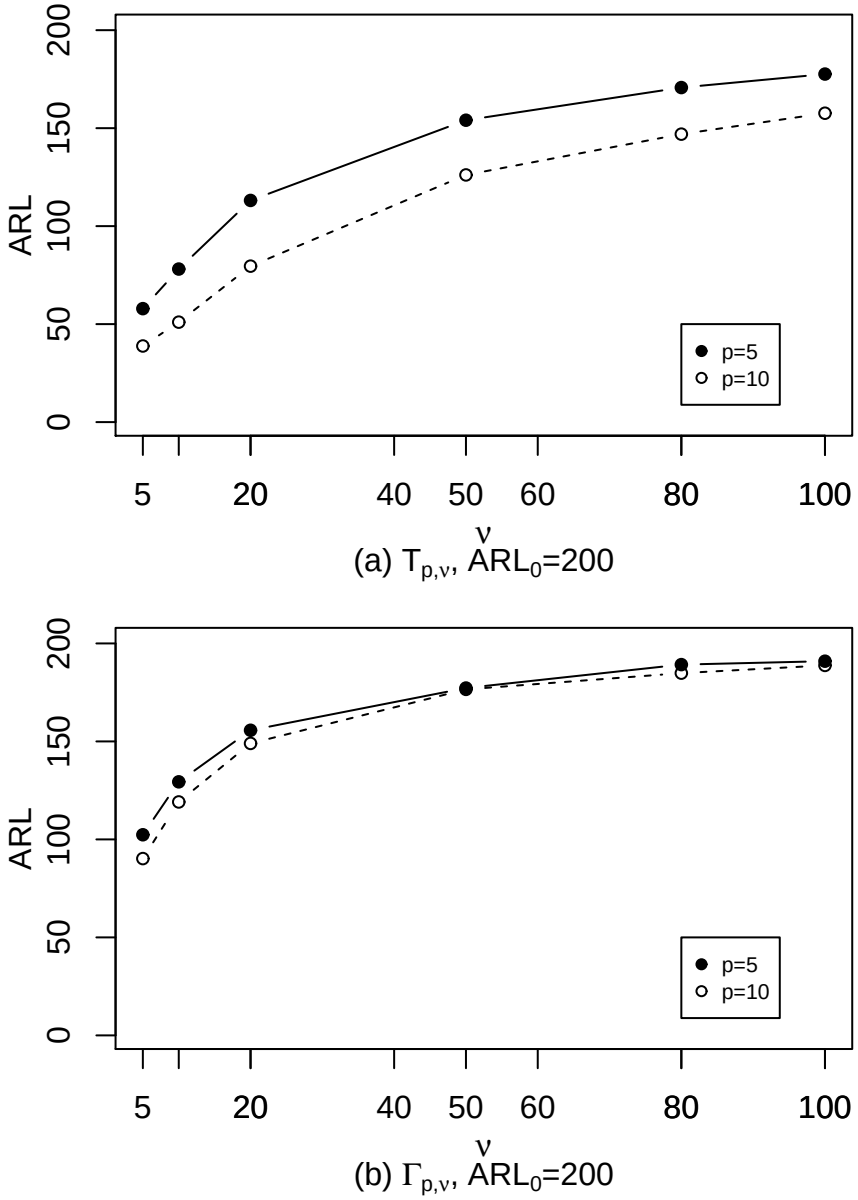


Fig. 1. Actual ARL values when the IC distribution is multivariate $T_{p,\nu}$ and $\Gamma_{p,\nu}$.

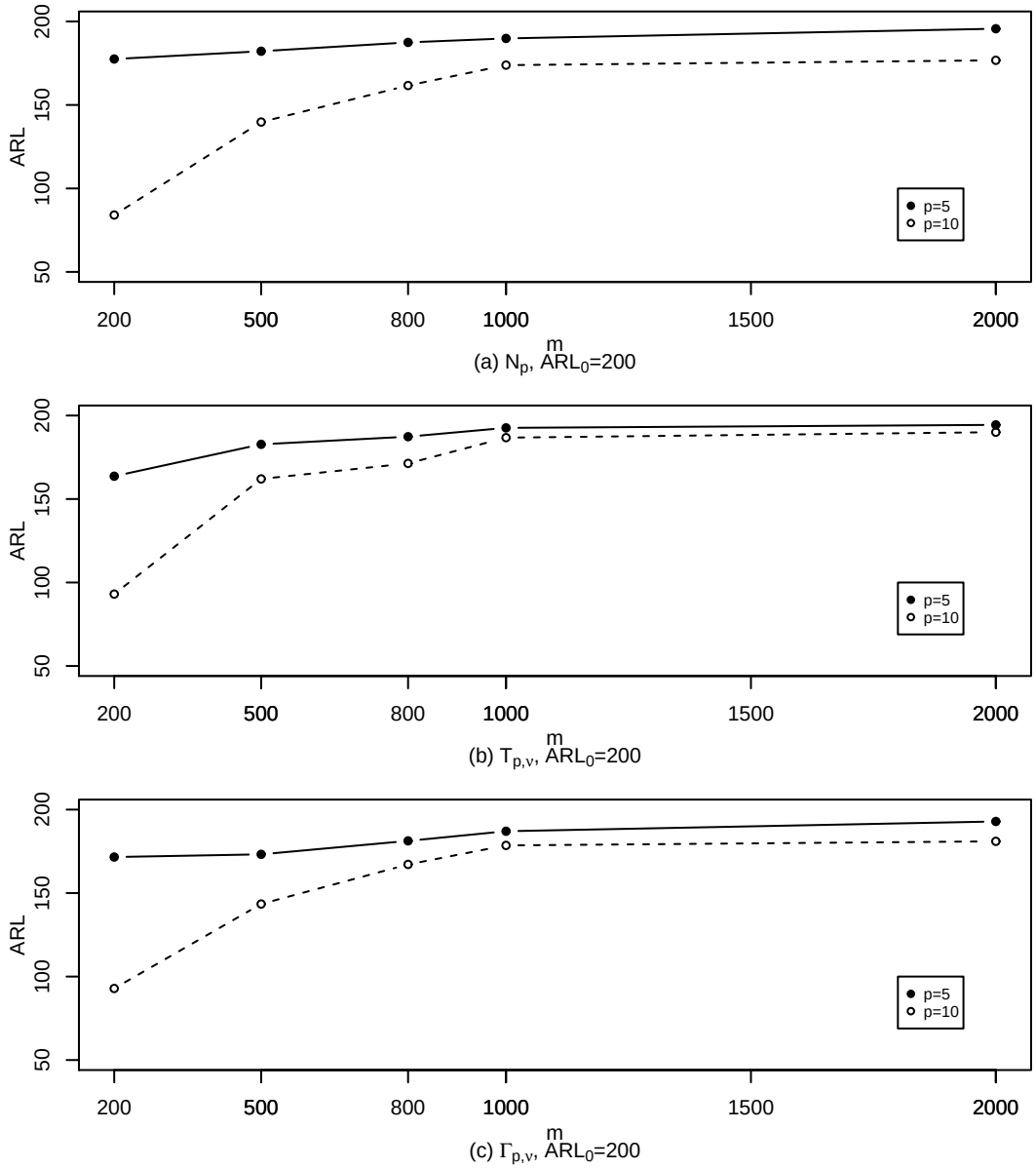


Fig. 2. Actual ARL values when the IC distribution is multivariate $N_p(\mathbf{0}, \mathbf{I}_p)$, $T_{p,\nu}$ and $\Gamma_{p,\nu}$.

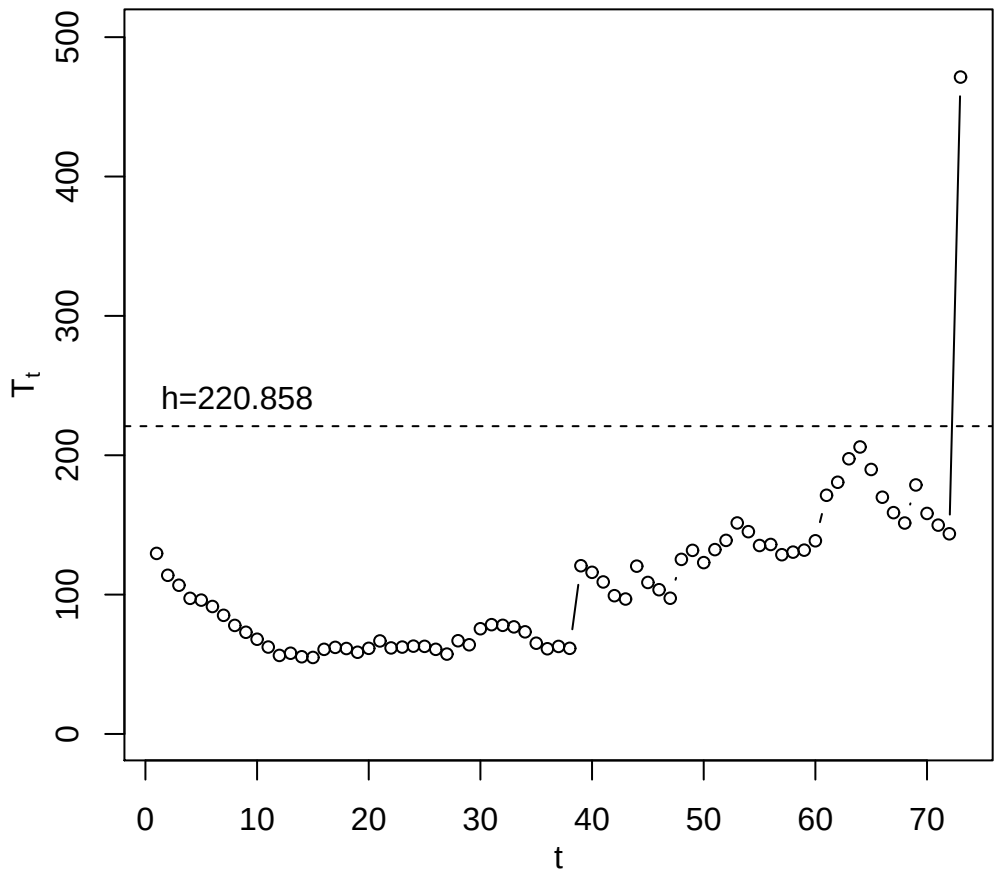


Fig. 3. The monitoring statistics of the MVP chart applied to the white wine production process.